

# Proton Predominance At UHE Cosmic Rays Through Analysis Of Different Mass Composition Models

Dr. Jyoti Prasad Phukan

Associate Professor, Department Of Physics

DHSK College, Dibrugarh, Assam, 786001

---

## Abstract

Recently, detection of giant ( $10^{17}$  to  $10^{20}$  eV) and super giant ( $E_p > 10^{20}$  eV) air showers is gaining importance as the investigation of EAS in these energy ranges is expected to give necessary information on characteristics of high energy nuclear interactions in one hand and for solving the astrophysical problem of Cosmic Ray origin, beyond the Greisen-Zatsepin-Kuzmin cut-off energy near  $10^{20}$  eV. Due to the very low Cosmic Ray flux in the UHE range ( $> 10^{17}$  eV) direct measurement by balloons or satellites are not possible. The experimental approach realized conventionally uses extended ground-based installations catching data of the induced air showers. An alternative approach is to use a low cost particle detector array called mini-array for detecting UHE cosmic rays by Linsley's method of arrival time measurement. The miniarray consist of eight plastic scintillation counters covering an area of  $2\text{m}^2$  operating for detecting EAS particles of primary energy  $10^{17}$  -  $10^{18}$  eV based on Linsley's method of arrival time measurement. An optical detector (5 inch diameter PMT) has been installed at the centre of the miniarray to record the associated optical Cerenkov pulse produced by the ultra-relativistic shower particles in the atmosphere with an aim to derive primary mass composition above  $10^{17}$  eV. Optical pulses are recorded in one channel of the DSO and the stored data in the wave form memory are transferred to the computer via GPIB interface. The particle detector pulses are triggered with the help of trigger circuit and recorded through other channel of the DSO and transferred to the same DSO. However, the data are subjected to large fluctuation both in particle detection and optical photon detection. Primary energy is estimated through the parameter shower size which is also indirectly measured from a small sample of shower front using miniarray data. Mass composition estimated indirectly relies on simulation model. On the basis of pulse height distribution measurement, the inferred mass composition is predominantly protons, with a tendency of mass composition becoming lighter at the highest energies.

**Keywords:** Extensive air showers, Ultra high energy, PMT, DSO, GPIB

---

Date of Submission: 10-10-2024

Date of Acceptance: 20-10-2024

---

## I. Introduction

It is well known that the slope of the lateral distribution of Cerenkov radiation is linearly related to depth of shower maximum and the rate of change of shower maximum with primary energy (elongation rate) is related to the change in primary mass composition. Hence, the Cerenkov light signal produced by shower electrons in the atmosphere provides a powerful technique to study the longitudinal cascade development and primary mass composition.

Optical pulses are recorded in association with G.U mini-array which records the arrival time spread (in nS) and charged particle density (in particle /  $\text{m}^2$ ) at the eight ( $50 \times 50 \times 5 \text{ cm}^3$ ) plastic scintillation counters covering carpet area  $2\text{m}^2$  at the roof top of the Physics Department. The measured time spread gives an estimate of the distance of the shower axis (Linsley's effect). The measured particle density when fitted to the lateral distribution function gives an estimate of the shower size and corresponding primary energy. The Cerenkov counter is located at the center of the mini-array. All the signals are amplified and carried to the control room via co-axial cables. Amplified scintillator pulses discriminated and OR'ed together to give a serial pulse train. This is branched into two channels, one going to the DSO for display and recording and the other going to the trigger circuit for generating the necessary trigger pulse. Particle pulses from the scintillation detector, associated Cerenkov pulses from the optical detector are recorded by the DSO and transferred to the computer via GPIB interface. The collected data are binned according to the measured shower size of each event. The slope of the curve between photon density and core distance in a log-log plot gives the exponent of the lateral distribution function.

## II. Data Acquisition System

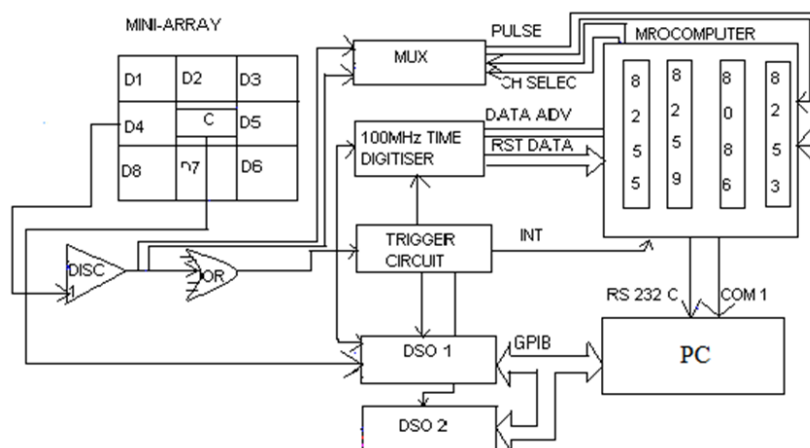


Fig.1-Block Diagram Of Experimental Set- Up.

Block diagram of the experimental set up for data acquisition is shown in fig.1. The event recording is handled by PC with GPIB interface. A microprocessor system is used (8086) to monitor the performance of the particle detector. Two DSO, Tektronix, TDS 520A & Tektronix, TDS 2024 record the particle pulses and associated Cerenkov and Radio pulses. Event trigger is generated by the trigger circuit which is explained below. Whenever trigger occurs recorded data in the oscilloscope is transferred to the computer via GPIB and store in disc. The recorded data is analyzed off line.

## III. Eight Channel Discriminator

A modified multi-channel discriminator board is designed and fabricated using high speed voltage comparators for the present experimental set up. The reference voltage is produced by the precision reference source RF01 and LM 301 and acts as discriminator level at the input of the comparator. The pulses from the detector are fed into the inverting input terminal of the high speed comparator U2 (LM 361) and the bias is set by the ten turn preset. As the incoming pulse crosses the discriminator bias in the comparator input, the unit produces the logic pulse. The circuit diagram of one channel of the discriminator with pulse shaper is shown in the figure 2.

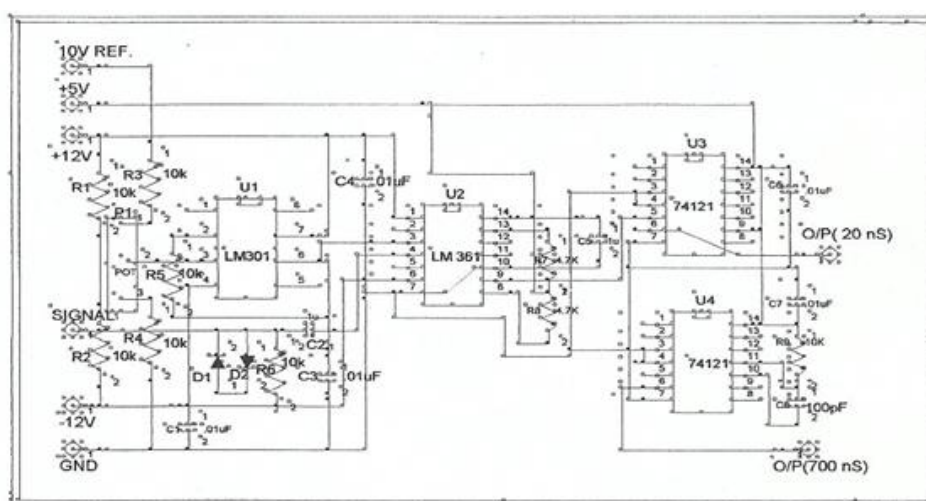


Fig.2- Circuit Diagram Of One Channel Discriminator With Pulse Shaper

The output of the discriminator is shaped into two separate pulse widths by using IC 3 and IC 4 (Mono stable Multivibrator). One of them is of 20nS which is used for recording of air shower events. The another one has pulse width 700nS. This pulse is generally used for counting purpose at a pre-determined intervals, controlled by the microprocessor 8086. Figure 3 shows the typical output pulses of the discriminator corresponding to an event trigger captured by the Digital Storage Oscilloscope. CH-1 shows the discriminator output while the CH-2 gives the trigger pulse.

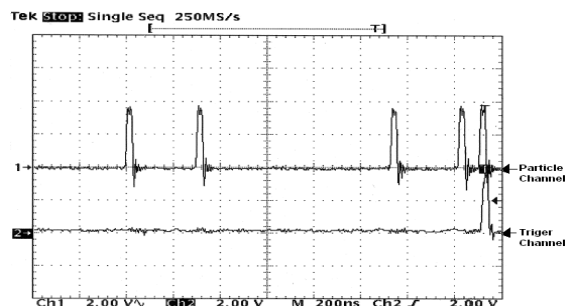


Fig.3-A Typical Output Pulses Of The Discriminator Corresponding To An Event Trigger.

#### IV. The Trigger Unit And Circuit Description

For recording optical pulse in association with UHE Cosmic Ray events, the wave forms are captured under some prerequisite criteria. These criteria's are -

- (a) The particle detector pulses are triggered by the Čerenkov pulse and must be present within the time window  $2\mu$  S.
- (b) The hardware trigger requiring particle in the range two or above within the  $2\mu$  S time window.
- (c) The minimum arrival time spread between the particles must be 100nS. The trigger unit is shown in fig.4.

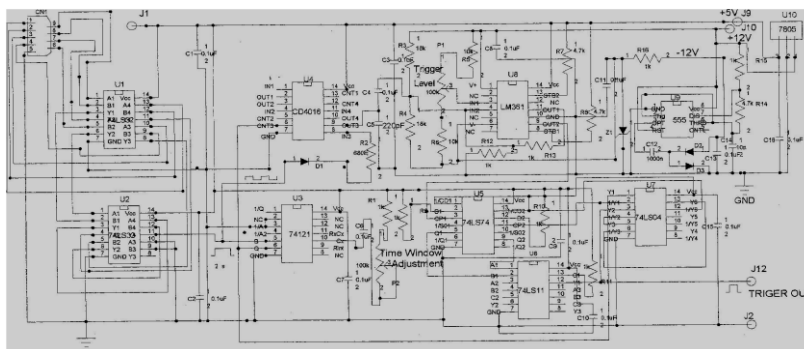


Fig.4-Schematic Diagram Of Trigger Circuit.

- (d) Optical pulse and particle detector pulses received within the  $2\mu$  S time window are recorded by capturing the waveforms displayed in the two channels of the DSO, channel one being used for optical and channel two for particle pulses. The trigger circuit design on an idea by and shown in the figure 4 performs the function required under criterion(b).The output pulse train from the OR gate charge the capacitor  $C_5(220\text{pF})$  through the diode  $D_1(\text{IN } 914)$  for a time period determined by the timing pulse at the CMOS Gate, U4 (4016-Quadruple Analog Switch). The timing pulse is generated by applying the pulse train to U3( 74121)which is at present set to  $2\mu\text{S}$  by preset  $P_2$ . The gate pulse discharges the capacitor at the end of  $2\mu\text{S}$  period. The voltage at the capacitor varies as the number of pulses received in the  $2\mu\text{S}$  duration. This voltage across C5 is fed to a high speed voltage comparator U8 (LM 361) and the trigger pulse is generated by the U5(74S74- Dual Edge Triggered Flip-Flop) and U6(74LS11- Triple 3- Input Positive-And Gate). The  $2\mu\text{S}$  Gate pulse is inverted and brought to the CLK2 input of the flip-flop and both the outputs are combined by U6 to ensure that the trigger pulse is generated at the end of the  $2\mu\text{S}$  time window.

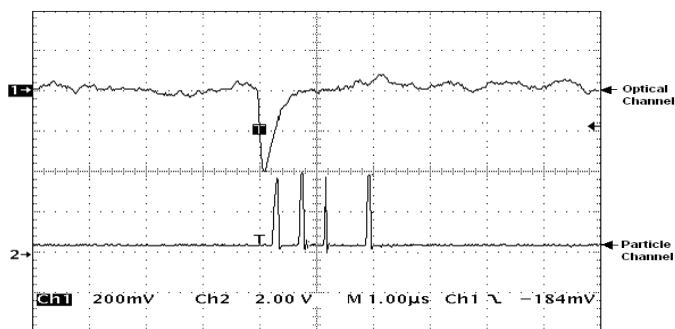


Fig.5- A Typical Čerenkov Pulse Triggered By Miniarray Trigger Is Captured By DSO.

From the recorded pulse height of the optical Čerenkov light, first the minimum and maximum heights are deduced using subroutine 'minmax'. These values are 50 mV and 940 mV respectively. The range of pulse height is therefore taken from 50mV to 950mV and divided into 18 number of class intervals each of size 50mV. The frequency of events in each bin is plotted against mean class intervals and compared with simulation results for four different mass composition models, viz., pure proton, pure iron, constant mixed and heavy to light.

To analyse the difference between each model calculation and the experimental data,  $\chi^2$  value is calculated for each case, taking the sum of  $\{(Y_{obs} - Y_{exp})^2 / Y_{exp}\}$ , where,  $Y_{obs}$  is observed (measured) frequency and  $Y_{exp}$  is the expected frequency from simulation under different composition models. per degree of freedom is the parameter, which has to be minimum for the best fit between calculated and measured data. The experimental pulse height distribution and  $\chi^2$  per degree of freedom are listed in table 1. Present analysis gives minimum value 16.25 for pure proton and a bit higher value,19.92 for a composition changing from heavy to lighter.

**Table 1 : Distribution of Čerenkov Pulse height and photon density**

Pulse height (mV)	Class mark (mV)	Čerenkovflux density (photons / m <sup>2</sup> ) ( $\times 10^4$ )	Frequency	Errors	$\chi^2 / df$ (model) Proton / Iron / CM / H to L	Remark
50 - 100	75	0.77	3	1.73		
100 - 150	125	1.27	10	3.16		
150 - 200	175	1.79	90	9.49		
200 - 250	225	2.3	83	9.11	16.25/ 47.58/ 36.83/ 19.92	Proton
250 - 300	275	2.81	41	6.4		Composition
300 - 350	325	3.32	31	5.57		Favoured
350 - 400	375	3.38	12	3.46		
400 - 450	425	4.44	17	4.12		
450 - 500	475	4.86	7	2.65		
500 - 550	525	5.54	2	1.41		
550 - 600	575	5.88	1	1		
600 - 650	625	6.57	4	2		
650 - 700	675	6.90	0	0		
700 - 750	725	7.41	0	0		
750 - 800	775	7.92	1	1		
800 - 850	825	8.61	0	0		
850 - 900	875	8.94	0	0		
900 - 950	925	9.45	1	1		

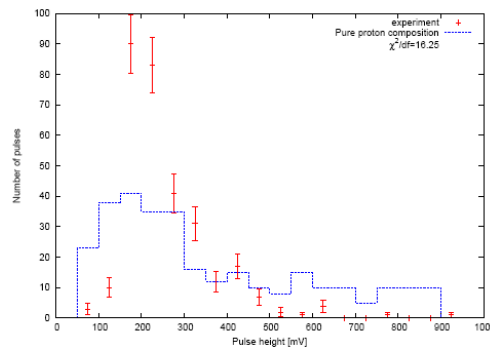


**Fig. 6.1: Čerenkov Pulse Height Spectrum For Pure Proton Composition Model.**

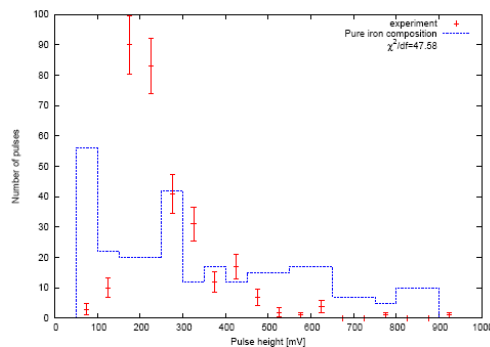


**Fig. 6.2: Čerenkov Pulse Height Spectrum For Pure Iron Composition Model.**

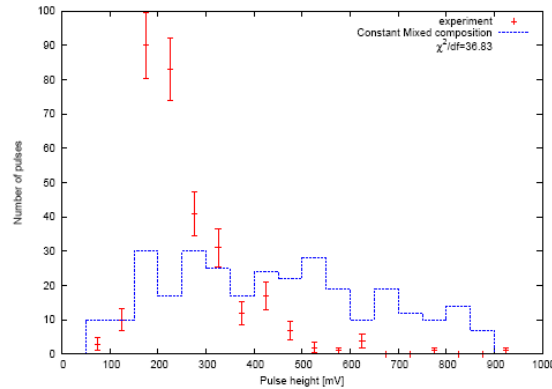


Fig.6.3: Čerenkov Pulse Height Spectrum For Constant-Mixed Composition Model.

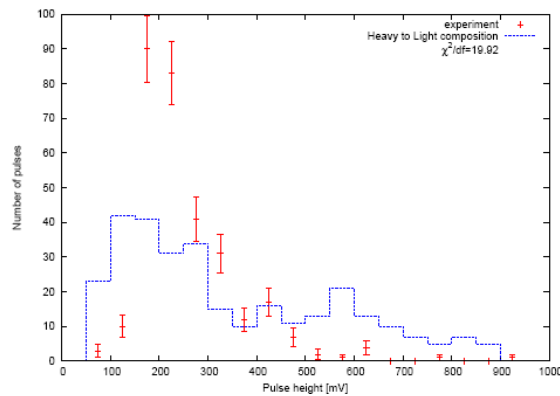


Fig.6.4: Čerenkov Pulse Height Spectrum For Heavy To Light Composition Model.

Comparison with simulation for four composition models are shown in fig. 6.1 to 6.4. Thus, based on pulse height distribution measurement, the inferred mass composition is predominantly protons, with a tendency of mass composition becoming lighter at the highest energies.

### Acknowledgement

The author thank the University Grants Commission (UGC), Govt. of India, for financial support under Minor Research Project and Department of Physics, Gauhati University, Guwahati, Assam for providing the data of cosmic ray event for this work.

### References

- [1] Gaurang B. Yodh, Review, Rapporteur And Highlight Paper, 29<sup>th</sup> ICRC, Pune, India, 2005, Vol.10, P.13-35.
- [2] Protheroe R.J. And Turever K.E. (1979), Nuo.Cim, 51A, 277.
- [3] Bezboruah T., Boruah K And Boruah P.K., (1999), Astroparticle Physics,
- [4] Phukan J.P., Boruah, K. And Boruah, K.B, 27<sup>th</sup> ICRC, Hamburg, Vol.2, P-407
- [5] Bezboruah T , Boruah K And Boruah P.K., (1998),NIM A 420,No.2,206.
- [6] Jelly J.V (1958) – Čerenkov Radiation And Its Applications, Ergamon Press, London.7.
- [7] O.Catalano,G.D.'Ali Staiti ,M.Gabriele And L.La Fata, Proc.27<sup>th</sup> ICRC, Hamburg, Vol.2, P-498.
- [8] Goswami, U. D. Boruah K And Boruah PK (2005), Astroparticle Physics 22, 421-429
- [9] Linsley, J. (1985).Proc.19<sup>th</sup> ICRC ,Lajolla,7,167.